DOI: 10.17587/mau.20.352-361

# Parametric Synthesis of the Control System of the Balancing Robot by the Numerical Optimization Method

**A. Yu. Ivoilov**[1], Ph. D. Student, iau13hv@mail.ru, **V. A. Zhmud**[1], D. Sc., Professor, oao_nips@bk.ru,
**V. G. Trubin**[1], Senior lecturer, trubin@ngs.ru, **H. Roth**[2], D. Sc., Professor, hubert.roth@uni-siegen.de,
[1]Novosibirsk State Technical University, Department of Automation, Novosibirsk, 630032, Russian Federation,
[2]University of Siegen, Department of Automatic Control Engineering, Siegen, Germany

*Corresponding author:* **Ivoilov Andrey Yu.,** Ph. D. Student,
Novosibirsk State Technical University, Novosibirsk, 630032, Russian Federation,
e-mail: iau13hv@mail.ru

*Accepted on February 15, 2019*

***Abstract***

*This article is devoted to parametric synthesis of a control system of a two-wheeled balancing robot. From the mathematical point of view, the robot is an inverted pendulum type object with a pivot point placed on the wheel axis. This device is unstable while de-energized. Devices of this type are excellent laboratory stands for testing and debugging control algorithms of unstable nonlinear systems. The inverted pendulum math model is well studied theoretically but, when designing a particular device many additional tasks arise such as taking into account the error in measuring the tilt angle and the influence of actuator nonlinearities. In this paper, one of these tasks is solved, namely, the problem of reducing the amplitude of the robot's oscillation around the equilibrium position. In practice, this oscillation almost always occurs in such systems and leads to various negative effects, such as increased energy consumption, increased wear of an actuator and heating of its windings, etc. Therefore, reducing the amplitude of the oscillation is an important task. To solve this task, the authors of the article propose to use the method of numerical optimization of the regulator, which is well recommended for solving many problems. The article analyzes the behavior of the device near the equilibrium position and identifies the causes of the self-oscillation. Further the method of its simulation is proposed. On the basis of numerical experiments, the main reason for the increase in the amplitude of the oscillation is revealed. The reason is an overlay of the reverse peak of the device transient process on the peak caused by a torque throw. The throw is generated by a combination of actuator backlash and static friction effects which cause the robot self-oscillation. The authors propose a technique of adjusting the regulator, aimed at reducing the magnitude of the reverse peak of the transition process and, as a consequence, reducing the amplitude of the oscillation. The effectiveness of the technique is confirmed experimentally by the results of numerical simulation of the robot's behavior and the results of testing the coefficients obtained in a real device. The use of the technique allowed reducing the oscillation amplitude in a real device by almost three times.*

***Keywords****: two-wheeled balancing robot, numerical optimization, design, control system, PID controller, inverted pendulum*

*For citation:*

**Ivoilov A. Yu., Zhmud V. A., Trubin V. G., Roth H.** Parametric Synthesis of the Control System of the Balancing Robot by the Numerical Optimization Method, *Mekhatronica, Avtomatizatsiya, Upravlenie*, 2019, vol. 20, no. 6, pp...

УДК 681.513.11 + 681.5.013

DOI: 10.17587/mau.20...

**А. Ю. Ивойлов**[1], аспирант, iau13hv@mail.ru, **В. А. Жмудь**[1], д-р техн. наук, проф., oao_nips@bk.ru,
**В. Г. Трубин**[1], старший преподаватель, trubin@ngs.ru, **H. Roth**[2], D. Sc., Professor, hubert.roth@uni-siegen.de,
[1] Новосибирский государственный технический университет, Новосибирск,
[2] University of Siegen, Department of Automatic Control Engineering Siegen, Germany

# Параметрический синтез системы управления балансирующего робота методом численной оптимизации

*Изучается вопрос параметрического синтеза системы управления двухколесного балансирующего робота. С математической точки зрения это устройство представляет собой объект вида "Перевернутый маятник" с точкой подвеса на оси колеса и в обесточенном состоянии неустойчиво. Устройства такого типа являются хорошими лабораторными стендами для испытания и отладки алгоритмов управления для неустойчивых нелинейных систем. Математическая модель перевернутого маятника хорошо изучена теоретически, но при проектировании конкретного устройства возникает множество дополнительных задач, таких как учет ошибки измерения угла наклона и влияние нелинейностей исполнительного механизма. В данной работе решается одна из таких задач, а именно — задача уменьшения амплитуды автоколебаний робота около положения равновесия. Эти колебания на практике практически всегда возникают в подобных системах и приводят к различным отрицательным эффектам, таким как повышенный расход энергии, повышенный износ исполнительного механизма, нагрев его обмоток и пр. Поэтому снижение амплитуды этих колебаний — важная задача. Для решения этой задачи авторами статьи предлагается использовать метод численной оптимизации регулятора, хорошо зарекомендовавший себя для решения многих задач. В статье проводится анализ поведения устройства около положения равновесия и выявляются причины возникновения автоколебаний. Далее предлагается способ моделирования автоколебаний. На основе численных экспериментов выявляется основная причина увеличения амплитуды этих колебаний — наложение обратного пика переходного процесса устройства на пик, вызванный броском момента, порожденного процессами, вызывающими автоколебания — сочетанием эффектов механического зазора двигателя (люфта) и трения покоя. Далее авторами предлагается методика настройки регулятора, направленная на уменьшение величины обратного пика переходного процесса и, как следствие, уменьшения амплитуды автоколебаний. Эффективность методики подтверждается экспериментально результатами численного моделирования поведения робота и результатами проверки полученных коэффициентов в реальном устройстве. Применение методики позволило уменьшить амплитуду колебаний в реальном устройстве почти в три раза.*

***Ключевые слова:*** *двухколесный балансирующий робот, численная оптимизация, конструкция, система управления, ПИД контроллер, перевернутый маятник*

## Introduction

The article is devoted to parametric synthesis of a control system of the two-wheeled balancing robot (TWBR). The task of controlling a TWBR is highly relevant in modern technology. This type of devices has high mobility and maneuverability and is able to operate autonomously. This allows them to be used for solving a number of tasks, such as load delivery and sampling from hard-to-reach places, conducting observations, photo and video filming. Two-wheeled robots can be used in various fields of human activity, such as eliminating the consequences of natural and man-made disasters, working in hazardous conditions, using them as human helpers in everyday life, etc. From a mathematical point of view, a TWBR belongs to the control objects of the inverted pendulum type. The task of stabilizing an inverted pendulum is one of classical problems in the control theory. The behavior of many technical systems, in one way or another, is described by a model of this class of control objects. In some cases, this model describes the behavior of a part of the system or the system behavior at some stage of work. The mathematical model of the inverted pendulum is applied in medicine; in particular, it is used in the study of the human musculoskeletal system. In addition, laboratory benches, which are based on the inverted pendulum model, are excellent platforms for testing and debugging various control algorithms and synthesis methods.

Today, to solve the problem of stabilizing two-wheeled robots, various control methods are used that can be divided into three groups: linear, non-linear, and non-classical. Linear methods include the pole placement method, control using the PID regulator or its modifications, as well as various versions of these methods using adaptive control. The pole place technique is applied by authors in [1—3]. Non-linear control of a TWBR based on sliding mode application is presented in paper [4]. In paper [5] a special non-linear block, non-linear disturbance observer, is proposed to apply for stabilizing of a two-wheeled robot. An example of non-classical methods is fuzzy logic control. Various versions of this method are presented in [6—8]. In addition, when designing a specific device, a number of tasks arise that require separate consideration. These tasks include: estimating the tilt angle of the robot relative to the vertical, estimating the rotation angle and angular speed of the wheels, analyzing the influence of nonlinearities and unaccounted features of the motors, suppressing undesirable oscillations and others. Often the solving some of these tasks may lead to the need to adjust the control method of the system. In particular, the analysis of the features of the based on MEMS sensors subsystem of estimating the robot tilt angle, showed that it is necessary to adjust the overall control system of the robot [9]. In more detail the control system of the robot will be considered further. In this article, the problem of reducing the amplitude of the self-oscillations of the robot is solved. At present, this issue has been studied worse compared to the above. From the existing solutions, for example, the energy relations proposed in [10] to reduce the amplitude of self-oscillations can be noted, as well as a hybrid regulator that takes into account the presence of backlash motors, presented in [11]. However, often this question is not considered separately by researchers. In practice, this oscillation almost always occurs in such systems and lead to various negative effects, such as increased energy consumption, increased wear of an actuator and heating of its windings, etc. Therefore, reducing the amplitude of the oscillation is an important task.

## The features of the TWBR

The appearance of the two-wheeled balancing robot is shown in Fig. 1. This device is a laboratory model of the vehicle "Segway". Structurally, the robot is designed as a platform to which the stators of DC motors are attached. A wheel with a tire is attached to the shaft of each motor. Boards with control and power electronics, as well as a battery that ensures autonomous operation of the device, are placed on the platform. The balancing robot is unstable in the de-energized state; an automatic stabilization system is implemented in the device to maintain balance by rotating the wheels. Fig. 2 shows the block diagram of the robot. The core of the device is the STM32F205 microcontroller of the 32-bit ARM architecture microcontroller family with the Cortex-M3 core. The microcontroller's control program performs a survey of the feedback sensors, calculates the control action applied to the DC motors, and sends the current values of the tilt angle of the robot, the rotation angle of the wheels and other data to the communication line. Two types of sensors are used to provide feedback in the robot: the MPU6050 measuring system, which is used to estimate the robot tilt angle and its derivative, and the quadrature optical encoders built into the DC motors, which are used to measure the rotation angle of the wheels relative to the robot body. The Lego NXT servomotors are used as actuators of the robot. The servomotors are permanent magnet DC motors. The rotation of the motors is controlled by the pulse-width modulation of the voltage applied to the motors windings. A bridge circuit is used to modulate the voltage of each motor. The circuit includes four field-effect transistors and their gates driver circuits. The device uses two lithium-

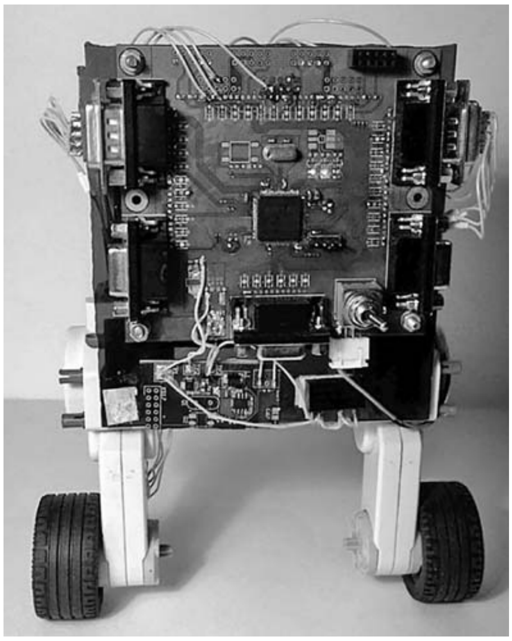

**Fig. 1. The two-wheeled balancing robot**

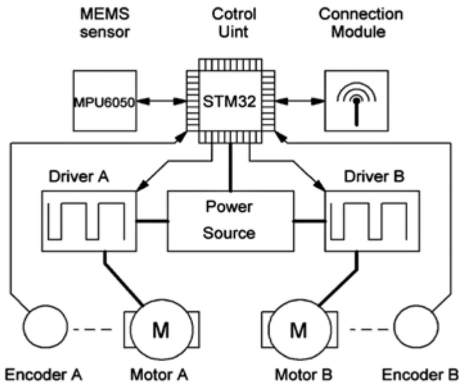


**Fig. 2. The block diagram of the robot**

ion batteries, connected in series, with a total voltage of 7.4—8.4 V, depending on the state of charge. To transfer data to an external computer, the device has an UART connector to which an USB-UART adapter for data transmission can be connected, or a Bluetooth module for wireless transmission.

## The control system of the TWBR

Let us to consider the automatic control system of the robot. The purpose of this system is to stabilize the robot in an upright position. In addition, this system eliminates uncontrolled movements of the robot in the horizontal plane. Mathematically, the two-wheel balancing robot is an object of the inverted pendulum type with a pivot point placed on the wheel rotation axle. The equations of motion of this object can be obtained on the basis of the Lagrange equation of the second kind [12]. We present a mathematical model of the robot in the form of transfer functions, obtained in [9]:

$$W_\varphi(s) = \frac{\varphi}{u} = \frac{k_o s}{s^3 + a_2 s^2 + a_1 s + a_0}; \quad (1)$$

$$W_\alpha(s) = \frac{\alpha}{\varphi} = k_\alpha \frac{s^2 + b_0}{s^2}. \quad (2)$$

The numerical values of the parameters of this model are shown in Table 1. The device control system is implemented in accordance with the structure shown in Fig. 3. Since the control system stabilizes both the tilt angle of the robot and its horizontal movements, the feedback system includes the robot's wheel rotation angle in addition to the tilt angle relative to the vertical. Each of these parameters has its own regulator; their transfer functions have the following form:

$$W_K(s) = \frac{u}{\varphi} = K_d s + K_p + \frac{K_i}{s}; \quad (3)$$

$$W_H(s) = \frac{u}{\alpha} = H_p + \frac{H_i}{s} + \frac{H_{ii}}{s^2}. \quad (4)$$

Here $\varphi$ is the robot tilt angle, $\alpha$ is the wheel rotation angle, $u$ is a voltage, applied to the motors windings. The regulator (3) is a PID regulator. The choice of the structure of the regulator (4) is due to the fact that a MEMS-gyroscope is used to measure the robot tilt angle and has the disadvantage of zero drift. The output value of the gyroscope is the angular velocity, i.e. the tilt angle derivative. On the one hand, this simplifies the implementation of the controller (3), since the derivative is available for direct measurement. On the other hand, to obtain the value of the robot tilt angle, it is required to integrate the gyroscope data, which leads to an accumulation of error. This is manifested in the fact that the value of the angle gradually "floats away", which over time leads to a loss of stability of the system. This effect can be considered as a linearly increasing tilt angle error. This error is represented in the block diagram as some $Err_g$ value, which goes to the input of the integrator.

In [9], it was shown that the structure described allows eliminating the negative effect of zero drift. The advantages of such a structure are higher performance, since the system does not apply filters for estimating values, and ease of implementation. However, the calculation of such a system is difficult, since it is necessary to calculate

Table 1

**The numerical values of the robots model parameters**

| Parameter | $k_o$ | $a_0$ | $a_1$ | $a_2$ | $k_\alpha$ | $b_0$ |
|---|---|---|---|---|---|---|
| Value | −2.8 | −490 | −52.3 | 9.9 | −7.07 | −49.5 |

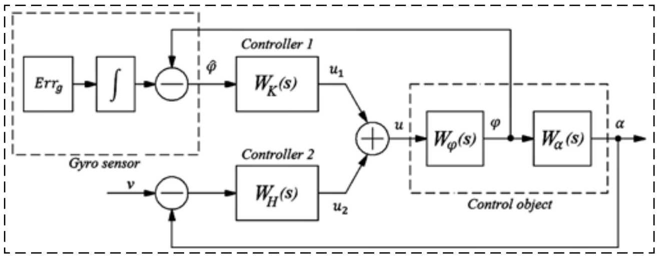


**Fig. 3. The structure of the robot's control system**

Table 2

**The regulators coefficients of the original system obtained in [13]**

| Coefficient | $K_i$ | $K_p$ | $K_d$ | $H_p$ | $H_i$ | $H_{ii}$ |
|---|---|---|---|---|---|---|
| Value | −4240 | −758 | −11.9 | −35.4 | −55.7 | −32.3 |

six coefficients. This means that when calculating the system, it is necessary to specify the closed loop system desired characteristic polynomial, which has the sixth order. This is difficult due to the presence of nonlinearities in the real device, such as dry friction and backlash of the motors, and limited control resource. Because of these effects, the choice of the desired polynomial is a non-trivial task, since in practice the system can become unstable even with the desired polynomial, giving a theoretically stable system [13]. In [13], the authors proposed a technique based on the numerical optimization method, which allows adjusting the coefficients of the control system regulators to obtain one or another form of transient processes, for example, with higher speed or with a lower level of oscillation. The values of the regulators coefficients obtained in [13] are presented in table 2. Fig. 4 shows graphs of the change in time of the robot tilt angle and wheel rotation angle.

As can be seen from the graphs, the control system solves the robot stabilization task. But in the real device there is self-oscillation around the

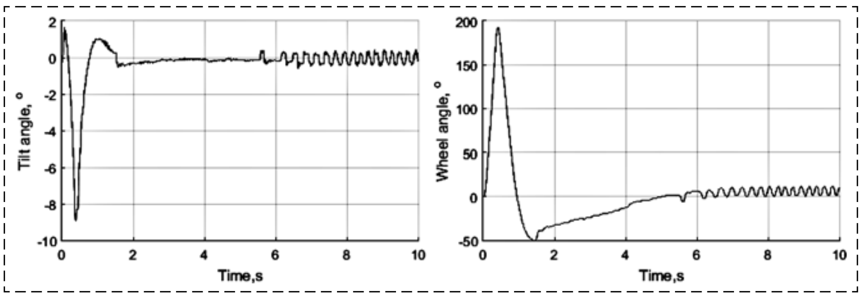


**Fig. 4. The original system: the tilt angle and the wheel angle**

equilibrium position. The peak-to-peak amplitude of the oscillation is about one degree, and the frequency is about 4 Hz. The presence of such oscillation is undesirable in view of the unnecessary battery power consumption, motors heating, etc. Therefore, it is necessary to eliminate these oscillations or, at least, significantly reduce their amplitude. It is also proposed to use the method of numerical optimization to solve this problem. Thus, the task of parametric synthesis of the robot control system is posed. To do this, it is necessary to solve two related tasks:

1) To propose a method of self-oscillation simulation;

2) To propose a technique of reducing the amplitude of self-oscillation based on the numerical optimization method.

## The Self-oscillation simulation

The most probable causes of self-oscillation in the real device are the presence of nonlinearities, which the current mathematical model of the robot does not take into account. First of all, this is a backlash of DC motors and dry friction, and the effect of static friction is most pronounced. Indeed, as can be seen from Fig. 4, oscillation begins only after the device's motors have completely stopped, and exactly at this point the change of direction of motor shaft rotation at which the backlash effect appears occurs. In the literature, one can find various recommendations on the simulation of backlash and friction of motors [17—21]. Five different variants of backlash simulation are described in [17]. Methods of compensation for the influence of backlash on motor control are proposed in [18] and [19]. However, in practice, simulation of these effects involves a number of difficulties. First, the simulation of the backlash in the composition of a particular system is complicated, since the model of the system is not continuous (for more details see below). Secondly, in order for the simulation results to be in accordance with the behavior of a real device, an experimental measurement of all necessary parameters is required, which can also be difficult. In addition, the values of these parameters may change during operation of the device. All this seriously complicates the application of modeling to the real device.

Let us to consider an alternative way to simulate the effect of the motor nonlinearities on the device behavior. The idea of the method lies in the fact that the self-oscillation itself is simulated (the consequence of backlash and friction phenomena) rather than the reasons for its occurrence. To do this it is necessary to select the correct model of

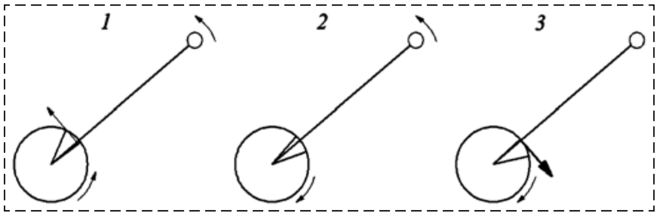


**Fig. 5. The movement of the system with backlash:**
*1* — the motor rotor and the load move together; *2* — independent movement of the rotor and the load after the changing the direction of rotation; *3* — the exit from the backlash zone

such oscillation. Let us to consider in more detail what happens with the system when changing the direction of wheel rotation. The motor rotor and the load move together before changing the rotation direction. When changing the direction of rotation, the load continues to move in the same direction, while the motor rotor moves in the opposite direction. Such movement is maintained for the time required for the rotor to overcome the mechanical gap. At this time, the system is uncontrollable, because the body of the robot is not connected to the motors shafts and hence to wheels. At the moment when the gap is passed, a short-term transient process occurs (in fact, a small blow), after which the load and the rotor move together. The above illustrates Fig. 5. From this we can conclude that the model of the robot is a piecewise function, its behavior is described by different models, depending on the current state. In addition, the system is also affected by the effect of static friction: when changing the direction of rotation, a slightly larger torque is required for the system to exit from the state of rest, compared with the torque of sliding friction. This excess torque is added to the hit torque arising from overcoming the mechanical gap, increasing the amplitude of oscillation.

Based on the above it is possible to propose to simulate self-oscillation as a series of periodic pulse disturbing influences:

$$M(t) = \left| \begin{array}{l} (-1)^n, t \in \left[ n\frac{T_M}{2}; n\frac{T_M}{2} + 0.01 \right] c \\ 0, t \in \left( n\frac{T_M}{2} + 0.01; (n+1)\frac{T_M}{2} \right) c \end{array} \right., \quad (5)$$

$$n = 0, 1, \ldots, \infty.$$

Here $T_m$ is a period of the pulse disturbance. It should be noted that such modeling is still estimated, since in a real system the parameters of self-oscillation, such as amplitude and frequency, depend on the parameters of the device, which means that resonance phenomena are possible. However, such modeling can be applied to study the causes of the increase in the amplitude of this oscillation. Let us to perform the oscillation simulation in system (1)—(4) with regulator parameters from table 2. We will simulate the oscillation in accordance with the expression (5) and set different values of the period of the pulse disturbance. The simulation result is presented in Fig. 6. It can be seen from the figure that the amplitude of oscillation varies depending on the period of the pulse disturbance. From the simulation results, it follows that the amplitude of the oscillation increases if the next pulse disturbance acts on the system at the moment when the system passes the reverse peak of the transient process from the previous disturbance. This leads to overlap of two effects and the amplitude of the peak increases. In a real system, this is likely to cause the system to reach a certain resonant oscillation frequency. Therefore, in order to reduce the amplitude of the oscillation, it is necessary to reduce the magnitude of the reverse peak of the system response to a pulse disturbance. This is a key point in carrying the numerical optimization.

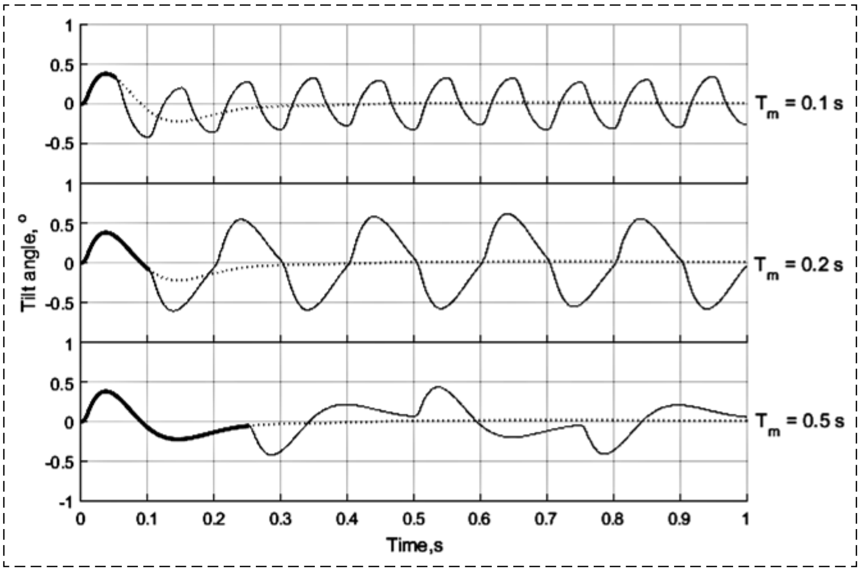


**Fig. 6. The robot self-oscillation simulation. Bold line depicts a part of the process before the second pulse of the disturbance influence. Dot line shows the system reaction on the non-periodical pulse disturbance**

### The regulator coefficients adjusting technique

Let us briefly consider the features of the numerical optimization method. The system model is complemented by some parameter called the system quality criterion. The value of this parameter indicates how close the system transient processes to the desired ones and is calculated by an expression called the cost function of the system. The smaller the value of the quality criterion, the better the processes in the system corresponds to the desired. A numerical simulation of the processes with certain initial values of the regulator coefficients is performed. Next, the values of the coefficients change in accordance with the optimization algorithm, and the system is resimulated. The simulation result, i.e. the value of the quality criterion is compared with the value in the previous step or several steps. Based on the results of this comparison, the values of the regulator coefficients change again, and the simulation is repeated, and so on. Thus, systems in which the quality of processes is worse are rejected, and those in which the quality is better are preserved. As a result, after a certain number of steps, the optimal values of the regulator coefficients are determined. The obtained coefficient values are used in a real device. Currently, these algorithms are implemented and successfully used in various software packages, such as *VisSim* or *Matlab*. The application of the numerical optimization method for solving a number of tasks is described in [14—16]. The cost function of the system can have a different form; its specific form is determined by the problem to be solved. An example of cost function is the following expression:

$$F_c(T) = \int_0^T |e(t)|^N \, t^R dt.$$

Here $e(t)$ is a control error, $t$ is time elapsed in the system, $T$ is total simulating time. As the time elapsed since the beginning of the transient process increases, the $t^R$ factor will make an increasing contribution to the cost function, which means that processes with lower speed will have a higher value of the quality criterion, and, therefore, will be discarded during optimization. In turn, the factor $|e(t)|^N$ is responsible for the overall value of the system error. As a result, by changing the values of the $R$ and $N$ coefficients, it is possible to obtain faster or less oscillatory processes, depending on the specific requirements. In [13], the following cost function was used to adjust the robot control system:

$$F_c(T) = \int_0^T |\dot{\alpha}(t)| \, t^4 dt. \tag{6}$$

Here, the wheel angular speed is selected as the control error, since to achieve equilibrium, not only maintaining the vertical position (i.e. zero value of the tilt angle) is required, but also the absence of uncontrolled horizontal movement (zero value of the wheel angular speed).

In order to reduce the reverse peak of the system response to the pulse disturbance, we introduce into the cost function (6) the additional term and take the values of the parameters $N$ and $R$ equal to 1:

$$F_c(T) = \int_0^T (|\dot{\alpha}(t)|t + 10^6 Q)dt, Q = \begin{vmatrix} 1, \varphi < -\varphi_{\text{lim}} \\ 0, \varphi \geqslant -\varphi_{\text{lim}} \end{vmatrix}$$

The purpose of this term is to dramatically increase the value of the cost function if the value of the tile angle exceeds a certain threshold determined by the value of $\varphi_{\text{lim}}$. In this case, such a process will be dropped during the automatic optimization procedure and, therefore, the reverse peak will be limited to $\varphi_{\text{lim}}$. In the course of optimization, we will model the response to a single (non-periodic) disturbing influence:

$$M(t) = \begin{vmatrix} 1, t \in [0; 0.01]c \\ 0, t > 0.01c \end{vmatrix}$$

The adjustment process, as in [13], is proposed to be divided into several stages. In this case, we will carry out the adjustment in three stages. The initial values of the coefficients $K_i$, $K_p$, $K_d$ are calculated on the basis of the block diagram of the simplified system presented in Fig. 7. The transfer function of the simplified system and the expressions for calculating the coefficients are as follows:

$$W_{simp}(s) = \frac{k_o(K_d s^2 + K_p s + K_i)}{s^3 + (a_2 + k_o K_d)s^2 + (a_1 + k_o K_p)s + (a_0 + k_o K_i)}; \quad (7)$$

$$a_2 + k_o K_d = a_2^*; \quad (8)$$

$$a_1 + k_o K_p = a_1^*; \quad (9)$$

$$a_0 + k_o K_i = a_0^*. \quad (10)$$

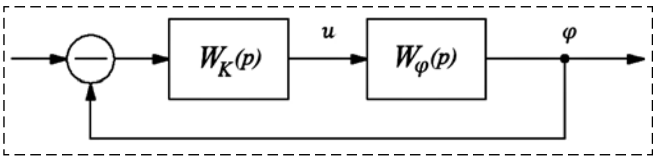


**Fig. 7. The block diagram of the simplified system**

Here $a_i^*$ is coefficients at the powers of s operator of the desired characteristic polynomial of the closed-loop system, which is required to calculate the regulator coefficients. Note that the simplified system is only needed to calculate the initial values of the coefficients.

At this stage, the regulator is optimized for an ideal device in ideal conditions. In practice, firstly, the device starts operation at a certain non-zero initial value of the tilt angle, and, secondly, the gyro error $Err_g$ is present in the system. At the first stage, both of these parameters are set equal to zero. At the second stage, the $H_p$ and $H_i$ coefficients are adjusted, and their initial values are set to zero. The purpose of this stage is to adjust the system response to non-zero initial conditions. Therefore, in the system a certain small initial value of the tilt angle is set; the error value of the gyroscope $Err_g$, as before, is set to zero. Note that it is also necessary to slightly reduce the requirement for the value of the reverse peak, since now the system also fulfills the initial condition in addition to pulse disturbance. Therefore, the value of the threshold $\varphi_{\text{lim}}$ must be reduced. In the third stage, the same coefficients are adjusted as in stage 2, but the coefficient $H_{ii}$ is also added to them. The purpose of this stage is to adjust the system when there is a gyroscope error. The initial value the tilt angle is set equal to zero, and the value of the gyroscope error is taken to be equal to a certain value determining the maximum rate of increase of the tilt angle error. Measurements in a real device show that this value is in the range of 0.18—0.23 °/*s*, therefore, we take a value with a margin of 0.25 °/*s*.

The results of the optimization, as well as the simulation conditions for each stage, are presented in Table 3. When calculating the initial values of

Table 3

**The results of the regulator coefficients adjustment**

| The stage number | | | 1 | | 2 | | 3 |
|---|---|---|---|---|---|---|---|
| The simulation time, *s* | | | 2 | | 5 | | 5 |
| The initial tilt angle, ° | | | 0 | | 0.1 | | 0 |
| The gyro sensor error, °/*s* | | | 0 | | 0 | | 0.25 |
| The tilt angle threshold ($\varphi_{\text{lim}}$), ° | | | −0.5 | | −0.7 | | −0.7 |
| The coefficients values: | Before | After | Before | After | Before | After | |
| $K_i$ | −9820 | −5030 | −5030 | −5030 | −5030 | **−5030** | |
| $K_p$ | −983 | −914 | −914 | −914 | −914 | **−914** | |
| $K_d$ | −28.6 | −28.2 | −28.2 | −28.2 | −28.2 | **−28.2** | |
| $H_p$ | — | — | 0 | −18.4 | −18.4 | **−23.2** | |
| $H_i$ | — | — | 0 | −47.3 | −47.3 | **−40.0** | |
| $H_{ii}$ | — | — | — | — | 0 | **−18.1** | |

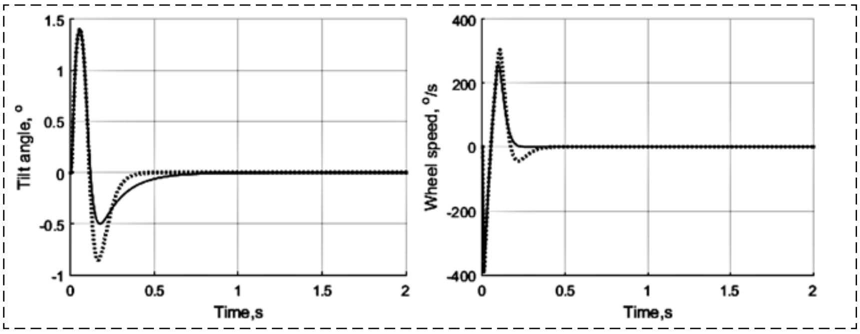


**Fig. 8. The result of the optimization at stage 1. Dot line depicts the system before adjustment; solid line shows the adjusted one**

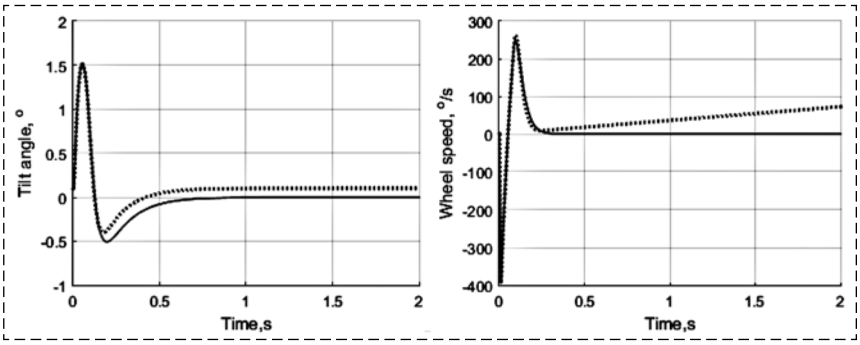


**Fig. 9. The result of the optimization at stage 2. Dot line depicts the system before adjustment; solid line shows the adjusted one**

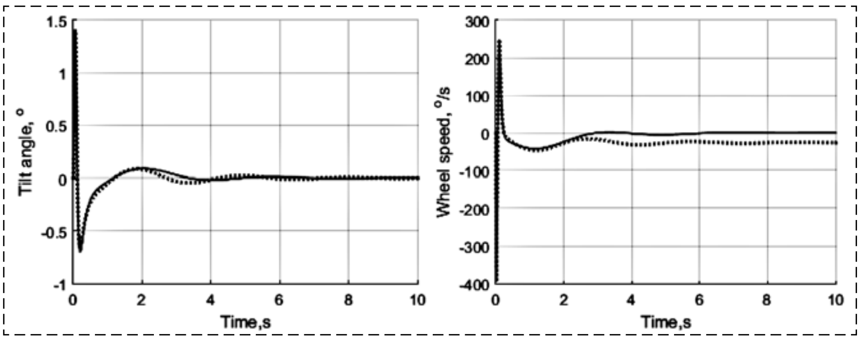


**Fig. 10. The result of the optimization at stage 3. Dot line depicts the system before adjustment; solid line shows the adjusted one**

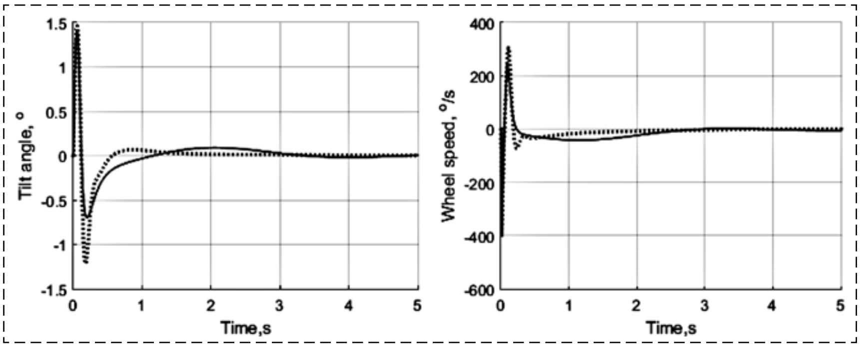


**Fig. 11. The simulation of the robot transient processes. Dot line depicts the original system with regulator coefficients form Table 2; solid line shows the adjusted one**

the coefficients, the following desired characteristic polynomial of the closed-loop system was used:

$$A(s) = (s+30)^3 = \\ = s^3 + 90s^2 + 2700s + 27\ 000.$$

Figures 8—10 show the transient processes of the system at each stage of adjustment. Fig. 11 shows the result of operation of the original (with the regulator coefficients from Table 2) and the adjusted systems. As it can be seen from the figure, the reverse peak was reduced by almost 2 times using the technique proposed, while slightly increasing the transient process time.

Perform a simulation of oscillations in the original and adjusted system. The simulation result is shown in Fig. 12. It can be seen from the figure that the amplitude of oscillation of the adjusted system was reduced by 1.5—2 times in comparison with the original system.

## Testing the technique in the real device

The regulator coefficients obtained during adjustment (see Table 3) were applied in the real device. The results of the operation of the balancing robot with the initial and adjusted coefficients of the regulators are presented in Fig. 13 and Fig. 14. Fig. 13 shows graph of the robot tilt angle upon completion of the transient process. From the figure it can be seen that the amplitude of self-oscillation has decreased by almost 3 times, compared with the original system; and the value of the mean square error in the adjusted system is almost 8 times lower: $7.58 \cdot 10^{-2}$ degrees for the original system and $1.03 \cdot 10^{-2}$ for the adjusted one. The transient process time of the tilt angle slightly increased, as can be seen from Fig. 14, while the same parameter for the wheel rotation angle process remained almost unchanged.

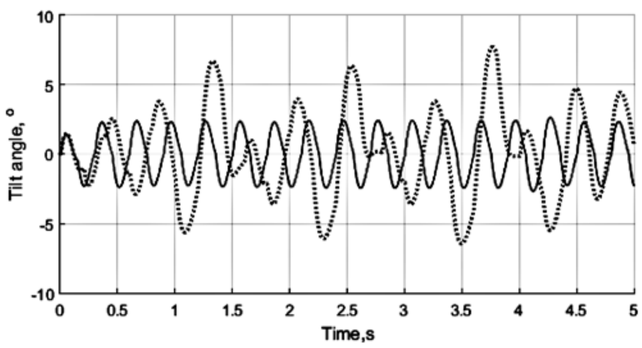


**Fig. 12. The simulation of the self-oscillation. Dot line depicts the original system; solid line shows the adjusted one**

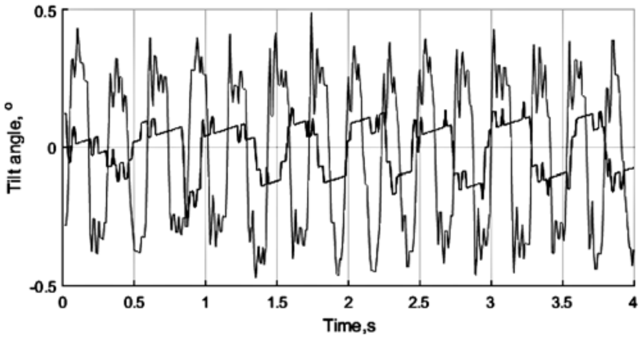


**Fig. 13. The robot self-oscillation. Gray line depicts the original system; black line shows the adjusted one**

## Conclusion

The objectives of the research are completed. The analysis of the causes of robot self-oscillation around the equilibrium position has been carried out. A method of the robot oscillation simulation is proposed, which consists in simulating the response of the system to a periodic pulse disturbance influence. Numerical experiments with the proposed model allowed us to reveal the main reason for the increase in the amplitude of self-oscillation, which consist of overlap of the peak caused by the system reaction on the pulse disturbance and the reverse peak caused by the reaction on the previous disturbance. Based on this, a three-step technique for adjusting the device regulator coefficients based on the method of numerical optimization is proposed. In the course of this technique, the system is optimized to reduce the magnitude of the reverse peak, which leads to a decrease in the amplitude of self-oscillations. The effectiveness of the technique is confirmed experimentally by the results of numerical simulation of the robot's behavior and the results of testing the coefficients obtained in the real device. The use of the technique allowed reducing the oscillation amplitude in the real device by almost three times. Thus, the proposed technique has shown its efficiency even when working with the real device.

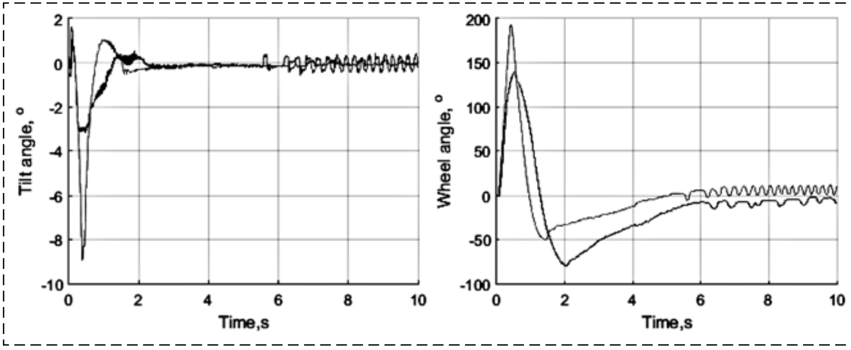


**Fig. 14. The robot transient processes. Gray line depicts the original system; black line shows the adjusted one**

### References


1. **Yamakawa S.** Tracking Control of Wheeled Inverted Pendulum Based on the Time-State Control Form, *Proceedings of the 18th World Congress of The International Federation of Automatic Control,* Milano, Italy. August 28 — September 2, 2011, pp. 10691—10696.

2. **Nawawi W. S.** Chapter 16 Real-Time Control System for a Two-Wheeled Inverted Pendulum Mobile Robot, Advanced Knowledge Application in Practice, Rijeka, IntechOpen, 2010, available at: https://doi.org/10.5772/10362.

3. **Mahmoud M. S., Nasir M. T.** Robust Control Design of Wheeled Inverted Pendulum Assistant Robot, *IEEE/CAA Journal of Automatica Sinica*, October 2017, vol. 4, no. 4, pp. 628—638.

4. **Xia D., Yao Y., Cheng L.** Indoor Autonomous Control of a Two-Wheeled Inverted Pendulum Vehicle Using Ultra Wide Band Technology, *Sensors (Basel)*, June 2017, vol. 17, no. 6.

5. **Ri S. H., Huang J., Wang Y., Tao C., Kim J. Y., Pak K. C.** Dynamic Surface Control of Mobile Wheeled Inverted Pendulum Systems with Nonlinear Disturbance Observer, *Proceedings of the 19th World Congress of The International Federation of Automatic Control,* Cape Town, South Africa. August 24—29, 2014, pp. 4505—4510.

6. **Kim H. W., Jung S.** Fuzzy Logic Application to a Two-wheel Mobile Robot for Balancing Control Performance, *International Journal of Fuzzy Logic and Intelligent Systems,* June 2012, vol. 12, no. 2, pp. 154—161.

7. **Wu J., Zhang W., Wang S.** A Two-Wheeled Self-Balancing Robot with the Fuzzy PD Control Method, *Mathematical Problems in Engineering*, 2012, vol. 2012, 13 pages, available at: https://doi.org/10.1155/2012/469491.

8. **Sangfeel K., Eunji S., Sik K. K., Seop S. B.** Design of Fuzzy Logic Controller for Inverted Pendulum-type Mobile Robot Using Smart In-Wheel Motor, *Indian Journal of Science and Technology*, March 2015, vol. 8, no. 5, pp. 187—196.

9. **Ivoilov A. Yu., Zhmud V. A., Trubin V. G.** The tilt angle estimation in the inverted pendulum stabilization task, *Proceedings of Moscow Workshop on Electronic and Networking Technologies (MWENT 2018)*, Moscow, Russia. March 14—16, 2018.

10. **Vasudevan H., Dollar A. M., Morrell J. B.** Design for Control of Wheeled Inverted Pendulum Platforms, *Journal of Mechanisms and Robotics*, November 2015, vol. 7, no. 4.

11. **Durdevic P., Yang Z.** Hybrid Control of a Two-Wheeled Automatic-Balancing Robot with Backlash Feature, *Proceedings of 2013 IEEE International Symposium on Safety, Security, and Rescue Robotics (SSRR)*, October 2013.

12. **Formal'skij A. M.** Upravlenije dvizhenijem neustojchivykh objectov (Control of unstable objects movement), Moscow, Phizmatlit, 2012 (in Russian).

13. **Ivoilov A. Yu., Zhmud V. A., Trubin V. G., Roth H.** Using the Numerical Optimization Method for Tuning the Regulator Coefficients of the Two-Wheeled Balancing Robot, *Proceedings of 14th International Conference on Actual Problems on Electronic Instrument Engineering (APEIE 2018),* Novosibirsk, Russia, October 2—4, 2018, pp. 228—236.

14. **Ivoilov A. Yu., Zhmud V. A., Roth H.** The Dynamic Accuracy Increasing for a Controlling System by Means of the Modified Algorithm of Numerical Optimization of the Regulator, *Proceedings of Moscow Workshop on Electronic and Networking Technologies (MWENT 2018)*, Moscow, Russia, March 14—16, 2018.

15. **Zhmud V. A., Dimitrov L. V., Yadrishnikov O. D.** Calculation of regulators for the problem of mechatronics by means of numerical optimization method, *Proceedings of 12th International Conference on Actual Problems on Electronic Instrument Engineering (APEIE 2014),* Novosibirsk, Russia, October 2-4, 2014, pp. 739—744.

16. **Zhmud V. A., Zavorin A. N.** The design of the control system for object with delay and interval-given parameters, *Proceedings of International Siberian conference on control and communications (SIBCON 2015),* Omsk, Russia, May 21—23, 2015, 6 p.

17. **Akoto C. L., Spangenberg H.** Modeling of backlash in drivetrains, *Proceedings of CEAS 2013 The International Conference of the European Aerospace Societies,* Linkoping, Sweden, September 2013, 11 p.

18. **Wu Yi., Wang Zh., Li Yu., Chen W., Du R., Chen Q.** Characteristic Modeling and Control of Servo Systems with Backlash and Friction, Mathematical Problems in Engineering, 2014, vol. 2014, 21 p. Available at: https://doi.org/10.1155/2014/328450.

19. **Prasanga K., Sariyildiz E., Ohnishi K.** Compensation of Backlash for Geared Drive Systems and Thrust Wires Used in Teleoperation, *IEEE Journal of Industry Applications,* 2015, vol. 4, no. 5, pp. 514—525.

20. **Papageorgiou D., Blanke M., Niemann H. H., Richter J. H.** Backlash estimation for industrial drive-train systems, *Preprints of the 20th World Congress, The International Federation of Automatic Control*, Toulouse, France, July 9—14, 2017, pp. 3336—3341.

21. **Hovland G., Hanssen S., Moberg S., Brogardh T., Gunnarsson S., Isaksson M.** Nonlinear Identification of Backlash in Robot Transmissions, *Proceedings of the 33rd ISR (International Symposium on Robotics)*, October 7—11, 2002.

## ВНИМАНИЮ АВТОРОВ

**Журнал "Мехатроника, автоматизация, управление"** входит в **ПЕРЕЧЕНЬ** рецензируемых научных изданий, в которых должны быть опубликованы основные научные результаты диссертаций на соискание ученой степени кандидата наук, на соискание ученой степени доктора наук, утвержденный ВАК, по следующим научным специальностям:

05.02.05 — Роботы, мехатроника и робототехнические системы (технические науки).

05.07.09 — Динамика, баллистика, управление движением летательных аппаратов (технические науки).

05.13.01 — Системный анализ, управление и обработка информации (по отраслям) (физико-математические науки).

05.13.01 — Системный анализ, управление и обработка информации (по отраслям) (технические науки).

05.13.06 — Автоматизация и управление технологическими процессами и производствами (по отраслям) (технические науки).